Journal of Theoretical and Applied Information Technology
15th May 2024. Vol.102. No 9

ISSN: 1992-8645 www.jatit.org E-ISSN: 1817-3195

SKIN LESION CLASSIFICATION FOR MELANOMA USING DEEP LEARNING

K SANDHYARANI KUNDRA[1], I V S VENUGOPAL[2], CH SITA KUMARI [3] , ANUSHA GUTTI [4]

[1,2] Information Technology, Gayatri Vidya Parishad College of Engineering (A), Andhra Pradesh, India
[3] Computer Science & Engineering, Gayatri Vidya Parishad College of Engineering (A), Andhra Pradesh, India
[4] Computer Applications, Gayatri Vidya Parishad College of Engineering (A), Andhra Pradesh, India

ABSTRACT

Deep learning is a branch of machine learning and Artificial Intelligence that imitates the way people learn specific types of information. Image classification is an area in Computer Vision where a computer can analyze an image and identify or estimate the probability of the class or category the image falls under. Melanoma has become more common over the past 30 years, and early detection has a big effect on lowering death rates from this type of skin cancer. The existing system consists of several physical laboratory test reports that are analyzed by a doctor or a cancer expert to detect the presence of melanoma. This alone is insufficient in countries with huge population like India, where cancer hospitals and labs are few. The proposed system consists of an image classifier that takes a dermatoscopic image as input and predicts whether a person has melanoma or not. A reliable automated system that can tell whether melanoma is present in a dermatoscopic image of lesions is a very helpful tool for medical diagnosis. This system uses an ISIC dataset specially curated for melanoma analysis. Thus, the proposed system serves as an automated, expedient, and practical method for detecting melanoma from the image of a skin lesion.
Keywords: *Computer Vision, Deep Learning, Image Classification, Machine Learning, Transfer Learning*

1. INTRODUCTION

Skin cancer refers to the abnormal expansion of skin cells that most typically occurs on sun-exposed skin. Unfortunately, areas of the skin that are exposed to sunlight may also acquire this type of cancer [1]. Skin cancer generally develops in areas of the body exposed to the sun, such as the scalp, face, lips, ears, neck, arms, etc. Moreover, it can also appear on regions of the body that receive minimal sunlight exposure, including the hands, the skin beneath the fingernails or toenails, and the genital area.

Skin cancer can affect all types of skin tones, although it is more common in individuals with darker skin tones. Melanoma is more inclined to appear on darker in complexion individuals in places like the soles of their feet and the palms of their hands that aren't regularly exposed to sun.

The three major kinds of skin cancer are melanoma, benign keratosis-like lesions, and melanocytic nevi. Early detection is required for these types of skin cancers, otherwise they can also affect other organs of the body.

Checking your skin for changes that look strange can help you find skin cancer early. Early detection of these cancers will improve the chances for successful treatment [2, 3]. The majority of the time, it is diagnosed visually. A clinical screening is the first step, followed by a dermatoscopic evaluation, a histological review, and a biopsy.

Even though it might be too late at times, the development of artificial intelligence and machine learning techniques holds the promise of significant time and error savings that could ultimately result in the saving of millions of lives.

In presenting our skin lesion classification system for melanoma using deep learning, it is imperative to delineate the scope within which our study operates. Our system addresses the critical need for accurate and efficient detection of melanoma, a formidable form of skin cancer, through the application of deep learning methodologies to dermatological image analysis. By focusing on melanoma detection, we aim to contribute to the advancement of early diagnosis, which is pivotal for improving patient outcomes and reducing mortality rates associated with this disease. Our work primarily revolves around the development and evaluation of a deep learning model trained on a curated dataset of skin lesion images, with a specific emphasis on melanoma classification. While our study is tailored to this particular

application, the methodologies and insights gained hold potential for broader implications in computer-aided diagnosis and medical imaging analysis.

2. LITERATURE REVIEW

Examining the skin for unusual changes is crucial for the early detection of skin cancer, enhancing the prospects of receiving effective treatment. Visual diagnosis, particularly for malignant melanoma, is the initial approach. Malignant melanoma has been persistently ranked as the most prevalent form of cancer in Australia, the United States, and Europe for an extended period. Early identification of this cancer significantly improves the chances of successful treatment, boasting a success rate of 92%. Although a biopsy is commonly employed to determine the malignancy or benignity of a tumor, the associated high costs and morbidity of laboratory procedures underscore the need for an alternative, equally prompt, and convenient screening method – an automated early detection system.

Numerous endeavors have been undertaken by researchers to create an automated system for skin cancer detection, aiming to enhance diagnostic accuracy. It is imperative to thoroughly examine the paths explored by these researchers in order to acquire substantial knowledge that can be instrumental in the development of a robust and effective skin cancer detection system. These approaches are discussed in the following literature. Dermatology imaging researchers think that melanoma diagnosis may be automated based on key physical traits and color details that are distinctive of skin cancer kinds. Lesioncolor, 3D form and size, and vertical thickness are all important melanoma diagnostic and prognostic criteria [2]. Traditional systems include various physical laboratory test reports which needs to be analyzed by a doctor or a cancer expert to detect the presence of melanoma [4].

Shetty et al. [5] presented a methodology for skin cancer identification using image detection techniques and computerized classification capabilities. To bolster robustness, their model incorporates k-fold cross-validation. The investigation assessed the accuracy in classification of both Machine Learning techniques and Convolutional Neural Network (CNN) techniques, indicating that CNN models demonstrated superior performance in terms of accuracy. The system attained an accuracy rate of approximately 95% with the CNN technique, enabling the proactive detection of distinct skin disease classes and empowering medical practitioners to prescribe appropriate treatments.

Md. Kamrul Hasan et al. [6] introduced a Dermoscopic Expert model, presenting an automated Skin Lesion Classification (SLC) framework that integrates a hybrid Convolutional Neural Network (hybrid-CNN) and advanced pre-processing techniques to generate intricate feature maps of skin lesions. Employing transfer learning from pre-existing models, their framework is designed for deployment in a web application, enhancing overall accuracy in skin lesion classification.

Ahmadi Mehr R et al. [7] suggested, a novel deep learning approach for the detection of skin cancer in lesion images. The method incorporated patient data, such as anatomical site, age, and gender, in addition to utilizing an Inception-ResNet-v2 Convolutional Neural Network (CNN) for effective recognition of objects. The model predicts the type of lesion not solely based on the lesion image but also considered relevant patient information. Their innovative approach has the potential to enhance the efficiency of skin cancer diagnosis by providing physicians with a more comprehensive set of data for analysis. The suggested technique enhanced the classification accuracy by 5% through the incorporation of patient metadata alongside lesion images, resulting in an accuracy of 89.3%±1.1% for distinguishing among four primary skin conditions and 94.5%±0.9% for discerning between benign and malignant lesions.

Detection of skin cancer traditionally relies on visual examination and dermoscopy, yet automated methodologies encounter difficulties such as artifacts, irregularities, and extractions of irrelevant features. Recent progress in deep learning, specifically leveraging convolutional neural networks (CNNs) with annotated skin images, demonstrate enhanced performance. S. P. Godlin Jasil et al. [8] study introduces a novel CNN architecture, combining Densenet and residual network, incorporating contextual data. The model underwent testing on the authoritative Human against Machine dataset (HAM10000) and was refined through up-sampling and additional information. The outcomes reveal a remarkable accuracy of 95% in the automatic classification of skin lesions.

Zillur Rahman et al. [9] in their investigation, introduced a novel weighted average ensemble learning model for the classification of skin lesions, leveraging the capabilities of five distinct deep neural network models. The model underwent training on a dataset comprising 18,730

dermoscopy images, with optimization focused on achieving an exemplary average recall score. The individual models demonstrated commendable performance, with ResNeXt, SeResNeXt, ResNet, Xception, and ResNet attaining recall scores of 88%, 89%, 91%, 88%, and 84%, respectively. Notably, the weighted average ensemble model achieved an impressive 94% recall, showcasing its efficacy in skin lesion classification.

Seeja R D et al. [10] primary objective of their research is to improve melanoma classification through the implementation of deep learning-based automatic skin lesion segmentation. The methodology involves the utilization of a Convolutional Neural Network (CNN) with the U-net algorithm for segmentation, extracting color, texture, and shape features through techniques such as LBP, EH, HOG, and Gabor. Subsequently, these features are input into classifiers, such as SVM, resulting in the attainment of a Dice coefficient value of 77.5%.

Adnan Afroz et al. [11] offered an analysis of various machine learning techniques for Skin lesion classification. The objective of their study is to assist examiners in developing proficient models for discerning between skin diseases and healthy skin images. It addresses challenges in skin tumor identification, explores pre-processing and segmentation techniques, provides comparisons with recent research, delves into classification methods, and explores the utilization of machine learning techniques. Additionally, the study scrutinizes the segmentation and classification processes utilizing the ISIC 2018 and 2019 datasets, highlighting challenges encountered in the analysis of skin diseases with these datasets.

Zahra Mirikharaji et al. [12] conducted a survey on skin lesion segmentation using deep learning methods. Their survey analyzed 177 research papers pertaining to the segmentation of skin lesions using deep learning techniques. The primary focus is on evaluating input data, model design, and assessment methodologies. The examination aims to elucidate the impact of these dimensions on current trends and suggests ways to overcome their limitations. The overarching goal is to alleviate the burden of skin cancer by addressing challenges related to both natural and artificial artifacts, intrinsic factors, and varying image acquisition conditions.

Drawing from parallel research findings, employing deep learning for skin lesion classification, specifically for melanoma, produces superior results. Consequently, the proposed system integrates deep learning methods with robust image processing techniques and decision-making processes to establish a computer-aided diagnostic system. This system aims to offer comprehensive methods facilitating the early detection of skin cancer. The innovative computer-aided diagnostic system, often denoted as computerized dermoscopy, has been developed.

Existing systems for skin lesion classification using melanoma detection methods rely heavily on manual analysis by medical professionals, leading to time-consuming and subjective diagnoses that are not scalable or accessible, particularly in underserved regions. Moreover, the subjectivity in diagnosis can result in inconsistencies and high false positive rates, causing unnecessary patient anxiety and healthcare costs. Insufficient training data and the inability of models to handle the variability in skin lesions further compromise the accuracy and reliability of existing systems. Additionally, the lack of real-time analysis capabilities limits the timely diagnosis and intervention crucial for improving patient outcomes. These pitfalls have been addressed in the proposed system necessitating the development of automated systems that are robust, scalable, and capable of accurately classifying melanoma from dermatoscopic images while being accessible to a wider population.

3. DATASET INFORMATION

The data utilized in this study is sourced from the global collaboration on skin imaging, specifically the International Skin Imaging Collaboration (ISIC). The dataset is composed of dermatoscopic images, serving as a comprehensive resource for training academic deep learning models. Within this dataset, a diverse range of pigmented tumors is featured, encompassing benign keratosis-like lesions such as solar lentigines, seborrheic keratosis, and lichen planus-like keratoses (BKL), as well as malignant entities like melanoma (Mel) and melanocytic nevi (NV).

Various independent variables are incorporated into the datasets, including but not limited to Image-id, lesion-id, and DX. These factors contribute as independent features in the analysis. The dependent variable, termed Outcome, is the target variable of interest. The Outcome variable is associated with cancer labels, providing a crucial focus for the investigation. This dataset thus presents a rich and diverse set of information for the development and training of deep learning models in the field of dermatoscopic image analysis.

The dataset encompasses a total of 10,116 images.

Figure 1 visually represents a selection of images extracted directly from this extensive dataset. The training dataset constitutes 80% of the overall data, while the testing dataset comprises the remaining 20%.

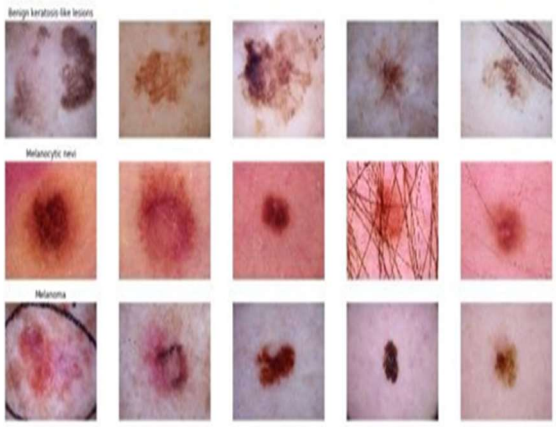

Figure. 1. Dataset Images

4. PROPOSED FRAMEWORK

The architecture for the proposed system is presented in Figure 2.

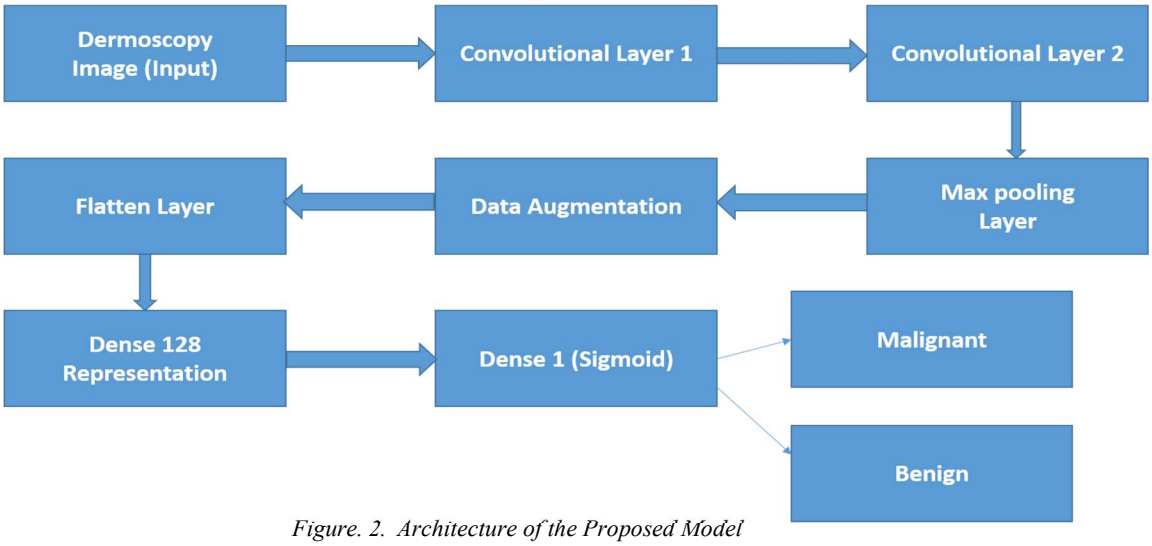

Figure. 2. Architecture of the Proposed Model

The architecture proposed in Figure. 2 includes the following components to automate the process of classification of melanoma:

- Convolutional layers with specified strides and zero padding.
- Max pooling layer for down-sampling.
- Data augmentation using ImageDataGenerator applied only to Melanoma pictures.
- Fully connected layers for classification.
- Output layer with a sigmoid activation function for binary classification

4.1. Convolutional Neural Networks

In feed-forward neural networks, the input layer neurons establish connections with every neuron in the output layer, forming what is commonly known as a fully connected (FC) layer. In contrast,

convolutional neural networks (CNNs) diverge from this architecture by avoiding the utilization of FC layers throughout most of the network, reserving them for the final layers. Consequently, it can be inferred that a CNN is a type of neural network where convolutional layers substitute for at least one of its conventional layers.

The outcomes of these convolutions undergo a non-linear activation function, such as RELU. To mitigate overfitting, convolutional RELU activation is applied before introducing one or two fully connected (FC) layers at the concluding stages of the network, culminating in the ultimate output classifications. This process helps in curbing overfitting by diminishing the width and height of the source volumes. Typically, a CNN employs hundreds or even thousands of filters on each layer, which subsequently consolidates the outcomes before transmitting the data to the subsequent layer. Throughout the training process, a CNN inherently acquires and refines the values associated with these filters [5, 6].

• Via the first stratum, edges are detected from the raw pixel data.
• Via the second stratum, the edges are used for detection of forms.
• Use these shapes to identify higher-level characteristics inthe network's upper layers.

The final layer of a CNN leverages these higher-level features to generate predictions regarding the content of the image. In practice, the compelling attributes of CNNs lie in their compositionality and local consistency. The principle of local invariance ensures that regardless of the object's placement in the image, its presence can be identified. The pooling layers play a key role in achieving local invariance by isolating regions in the input volume that exhibit a strong response to a specific filter.

Convolutional neural networks can be constructed with various levels, but the most commonly encountered ones include:

- Convolutional layer
- Pooling layer
- Dense layer
- Dropout layer

4.2. Convolutional Layer

The core of a CNN is its CONV layer, as indicated by previous research [4, 5]. Within this layer, the essential components are K learnable filters, commonly known as "kernels." These kernels are defined by both their width and height, with a typical configuration being square in shape. Despite their relatively modest spatial dimensions, these filters span the entire depth of the volume, contributing to their comprehensive influence on the input data.

The depth of a CNN is contingent upon the number of channels within its input feed, for instance, a depth of three when processing RGB images, signifying one channel for each color. Additionally, the depth of network volumes is intricately connected to the quantity of filters implemented in the preceding layer.

To enhance comprehension of this concept, let's delve into the forward-pass of a CNN. During this process, each of the K filters conducts convolutions both horizontally and vertically across the dimensions of the source volume. Alternatively, envision each of the K kernels sliding through the source area, executing element-wise multiplication, aggregating the results, and then storing the output value in the activation map in two dimensions, as depicted below:

Step 1: The K kernels are poised for application to the image.
Step 2: Each kernel engages in convolution with the input volume.
Step 3: The outcome of each convolution operation manifests as a two-dimensional output.

Hence, each entry in the output signifies the outcome within a neuron, considering only a small portion of information. As a result, the system evolves filters that activate when a specific characteristic is identified at a particular spatial location within the source volume. For instance, lower-level filters in the system can become active when detecting regions resembling edges or corners. Subsequently, the presence of higher-level features, such as components of a face, a car's hood, and similar intricate elements, can trigger filters at the deeper layers of the network. In our analogy of a neural network, this concept of activation aligns with the way neurons become stimulated and engaged when they recognize a specific pattern in an input image.

Efficiently combining a small filter with a large input volume holds particular significance in convolutional neural networks (CNNs), where the proximity of connections and receptive fields for each neuron is crucial. Given the multitude of connections and weights inherent in image processing, establishing connections between every neuron in the current volume and every neuron in the preceding volume can become impractical. Consequently, training deep networks on images with excessively large spatial dimensions becomes unfeasible. Instead, a strategic approach involves linking each neuron to a minute segment of the input

volume, termed the neuron's receptive field.
To illustrate this concept, consider a dataset with an input volume of 32x32x3, where each image has dimensions of 32 pixels in width, 32 pixels in height, and 3 pixels in depth. If the receptive field is set at 3x3, the CONV layer will generate a total of 3x3x3=27 weights. The depth of the filters is set at three, corresponding to the three channels encompassed by the source image in this scenario [7].
Until now, we've explored how neurons are interconnected at the input level, but we haven't delved into the specifics of how large or the manner in which the output level is shaped. The dimensions of the output volume are influenced by the size of the kernel, the stride size, and the zero-padding size.

4.3. Kernel

A filter, often referred to as a kernel, plays a crucial role in layered designs. It constitutes a smaller matrix with real-valued entries in contrast to the size of the image. Subsequently, activation maps are generated by convolving these kernels with the input volume. Activation maps visually highlight activated areas, indicating regions where the input exhibits properties specific to the applied kernel.

4.4. Stride

To execute a convolution, a small matrix is systematically moved over a larger matrix, halting at each point to conduct element-by-element multiplication and addition, followed by storing the resultant matrices. This process closely resembles a sliding window traversing an image horizontally and vertically, capturing information as it moves from left to right and top to bottom.

4.5. Zero Padding

To preserve the original size of an image post-convolution, it's necessary to apply "padding" to the outermost regions of the image. This consideration holds true for filters within a CNN as well. Utilizing zero-padding along the input's border ensures an exact match between the output volume and the input volume. The extent of padding is determined by the input "padding" parameter.
This strategy becomes particularly crucial in the context of deep CNN designs that incorporate numerous stacked CONV filters. To exemplify the concept of zero-padding, we applied a 3x3 kernel to a 5x5 input image with a stride of 1. As depicted in Figure. 3, the results showcase the impact of zero-padding.

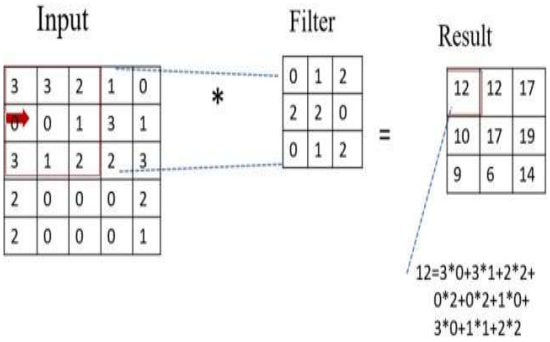

Figure. 3. Zero Padding Illustration

4.6. Pooling Layer

Two techniques for downsizing an input volume are POOL layers and CONV layers with a stride greater than one, as demonstrated. In the architecture of CNNs, POOL layers are commonly integrated between consecutive layers. The primary objective of a POOL layer is to gradually reduce the dimensions of the source volume, specifically its width and height. This reduction in complexity aids in diminishing the number of metrics and computations required, contributing to a more manageable system. Additionally, pooling plays a role in managing overfitting by consolidating processing and parameter data within the network.
POOL layers employ either the max or average function to operate on each input depth slice independently. Average pooling is often employed as the last layer of a network, especially in scenarios where there are no fully connected (FC) layers. On the other hand, max pooling is frequently implemented in the core of CNN designs to effectively reduce the overall size of the network.
The pooling layer encompasses two types of pooling techniques:

- MAX POOLING: This technique concentrates on the specific location where the weighted pixel is most pronounced in a given spot.
- AVG POOLING: In contrast, average pooling considers the entire image, with pixels dispersed across the entire picture. Figure. 4 illustrates the outcomes of average pooling.

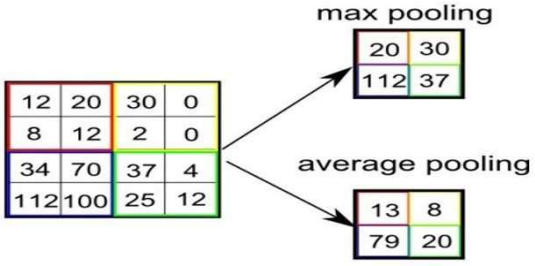

Figure. 4. Pool types

4.7. Fully Connected (Fc) Layer

Neurons within fully connected (FC) layers establish connections with all activations in the preceding layer, adhering to the conventional structure of feedforward neural networks. Towards the network's conclusion, FC layers are consistently integrated, avoiding a sequence where a convolutional (CONV) layer is succeeded by an FC layer, followed by another CONV layer. In a simplified architecture, multiple FC layers are typically employed before reaching the SoftMax classifier. This classifier, which determines the total output probabilities for each class, follows the (implied) SoftMax classifier. Preceding the SoftMax classifier, two fully connected layers are utilized. Figure. 5 provides a visual representation of the outcomes of a fully connected layer.

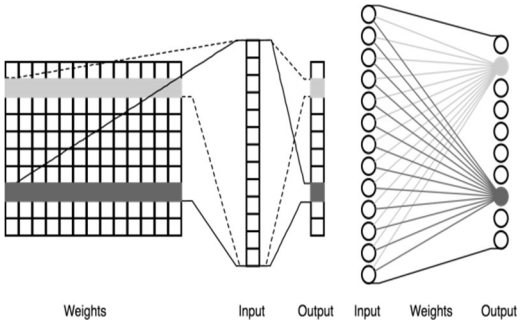

Figure. 5. Fully connected layer

4.7.1. CNN without Augmentation

Data augmentation involves employing various techniques to artificially expand a dataset by introducing additional data points. The objective is to augment the overall quantity of the dataset. This can be achieved through inconspicuous modifications to the existing data or leveraging deep learning algorithms to produce novel information. In the case of this model, no additions were made to the image library by the system.

4.7.2. CNN with Augmentation

Data augmentation encompasses a collection of techniques crafted to artificially enrich a dataset by introducing additional data points, thereby increasing the overall quantity of the data. This can be achieved through subtle modifications to the existing data or by utilizing deep learning models deep learning algorithms to produce novel information. In the context of this model, the augmentation has been applied to every image in the dataset.

4.7.3. CNN with Augmentation is applied only to theMelanoma Picture

Data augmentation encompasses the use of various methods to artificially enrich a dataset by incorporating additional data points, thereby augmenting the overall quantity of the dataset. This can involve inconspicuous alterations to existing data or the use of deep learning algorithms to produce novel information. In the context of model, the algorithm selectively applies augmentation only to the few melanoma images within the collection.

5. RESULTS AND ANALYSIS

To assess and comprehend the performance of the model under consideration, accuracy and loss graphs, as well as ROC curves are analyzed in section 5.1 and 5.2 respectively. These tools serve as essential tools for diagnosing the issues, optimizing model training, and evaluating the overall performance of skin lesion classification models. They provided valuable insights for making informed decisions about model adjustments and comparing different models.

5.1. Model accuracy and loss graph

- The suggested model's accuracy is denoted by the percentage of correct predictions it makes.
- The loss curve illustrates the model's error, providing insights into its performance. It quantifies how effectively or ineffectively the model is performing.
- The model underwent validation for 25 epochs. The blue curve depicts the performance on the training data, while the orange curve represents the performance on the validation data.

5.1.1. CNN Accuracy and Loss without Augmentation

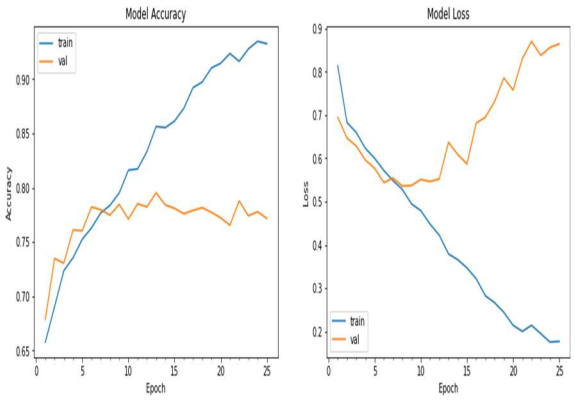

Figure. 6. CNN Accuracy and Loss without Augmentation

Journal of Theoretical and Applied Information Technology
15th May 2024. Vol.102. No 9

ISSN: 1992-8645 www.jatit.org E-ISSN: 1817-3195

In Figure 6, the y-axis corresponds to the precision rate, while the x-axis shows how many epochs there are in total. The blue line on the graph signifies the training score, and the orange line represents the epoch count. At this juncture, the accuracy stands at a higher value (0.93), and further increasing the number of training instances may lead the CNN to underfit the dataset.

5.1.2. CNN Accuracy and Loss with Augmentation

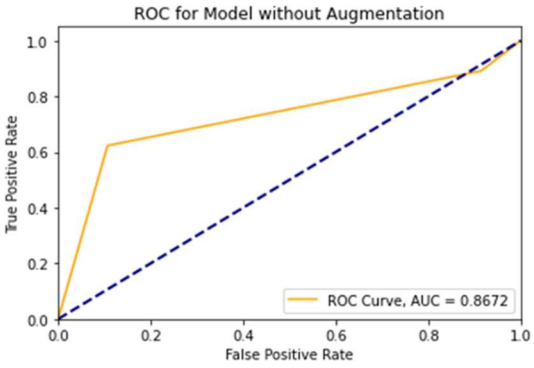

Figure. 7. CNN Accuracy and Loss with Augmentation

In Figure 7, the y-axis denotes the precision rating, and the x-axis shows how many epochs there are in total.. The blue line on the chart reflects the training score, while the orange line corresponds to the epoch count. At this specific juncture, the accuracy registers a higher value (0.74), and further increasing the number of training instances may potentially lead the CNN to underfit the dataset.

5.1.3. CNN Accuracy and Loss with Augmentation is applied only to Melanoma Picture

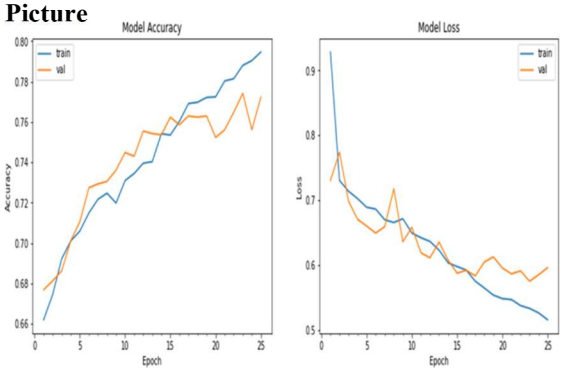

Figure. 8. CNN Accuracy and Loss with Augmentation is Applied only to Melanoma Picture

In Figure 8, the y-axis illustrates the precision rating, while the x-axis shows how many epochs there are in total.. The blue line in the chart corresponds to the training score, and the orange line signifies the epoch count. Notably, the accuracy reaches a higher value at this juncture (0.83), and there is a possibility that further increasing the number of training instances may lead the CNN to underfit our dataset.

5.2. ROC Curves

• The Receiver Operating Characteristics (ROC) curve illustrates the true positive rate versus the false positive rate across various categorization thresholds.

• In the subsequent graphs, the orange curves depict the performance of our model under different decision-rule settings, effectively identifying genuine positive values from fake positive ones. The ROC accuracy, represented by the blue line, is calculated based on the distance between the model performance curve and the linear.

5.2.1. CNN ROC without Augmentation

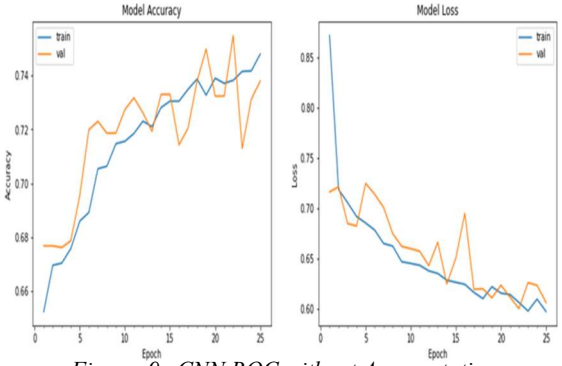

Figure. 9. CNN ROC without Augmentation

Figure 9 above illustrates the true positive score at different decision rules on the y-axis and the false positive rate score on the x-axis, representing thresholds. The model's effectiveness is depicted by the orange line, which forms the Receiver Operating Characteristics (ROC) curve, while the baseline is represented in blue. The computation of the ROC score relies on the area beneath the ROC curve, and in this case, the model's ROC value is 0.8672.

5.2.2. CNN ROC without Augmentation

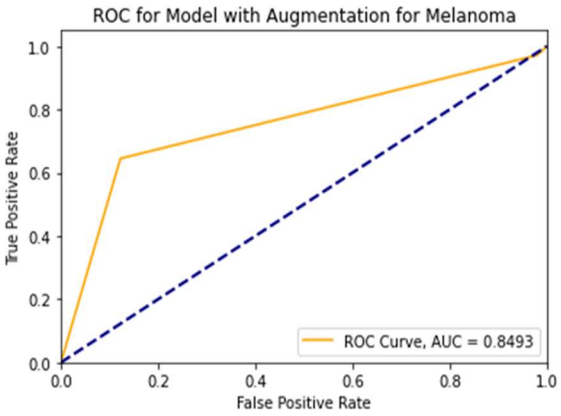

Figure. 10. CNN ROC with Augmentation

Figure 10 above illustrates the true positive score at different decision rules on the y-axis and the false positive rate score on the x-axis, representing thresholds. The model's effectiveness is depicted by the orange line, which forms the Receiver Operating Characteristics (ROC) curve, while the baseline is represented in blue. The computation of the ROC score relies on the area beneath the ROC curve, and in this instance, the model's ROC score is determined to be 0.8579.

5.2.3. CNN ROC with Augmentation is applied only to Melanoma Picture

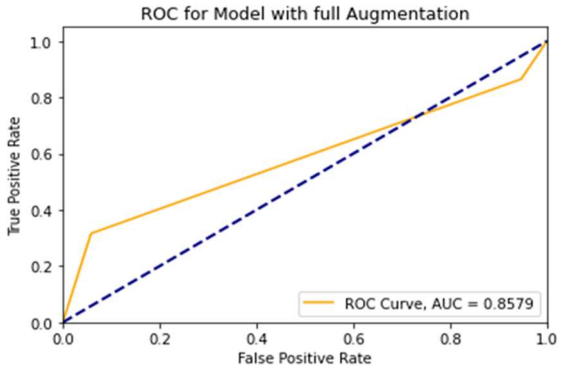

Figure. 11. CNN ROC with augmentation is only applied to melanoma picture

Figure 11 above displays the true positive score at different decision rules plotted against the false positive rate score on the x-axis, representing thresholds. The orange line on the Receiver Operating Characteristics (ROC) curve illustrates the effectiveness of our algorithm, while the baseline is depicted in blue. The ROC score is computed based on the area beneath the ROC curve, and in this instance, the model's ROC score is determined to be 0.8493.

The performance of the proposed model is shown in Table 1

Table 1. Model Performance

CNN	ACCURACY	ROC ACCURACY
WITHOUT AUGMENTATION	0.93	0.86
WITH AUGMENTATION	0.74	0.85
AUGMENTATION FOR MELONOMA PICTURES ONLY	0.83	0.84

Analysis from Table 1 indicates that the CNN model without augmentation yielded the highest accuracy, implying that, in this particular case, augmentation may not have conferred significant benefits. The observed decrease in accuracy with general augmentation can be attributed to the introduction of augmented data that deviates from the distribution of non-augmented data. Notably, the strategy of exclusively applying augmentation to Melanoma pictures has demonstrated improvement compared to general augmentation.

6. CONCLUSION

This study explored the integration of deep learning techniques, particularly through image classification in the realm of computer vision, offering a promising avenue for enhancing early detection of melanoma. The proposed automated system, leveraging dermatoscopic image analysis and a curated dataset tailored for melanoma detection, represents a significant step towards addressing the challenges posed by existing reliance on physical laboratory tests and manual analysis. By providing a reliable, expedient, and practical method for identifying melanoma from skin lesion images, this system holds substantial potential to improve medical diagnosis, particularly in areas where resources are constrained. The methodology involved constructing a Convolutional Neural Network (CNN) model, training and evaluating it. The developed approach achieved an accuracy of 84%.

7. FUTURE SCOPE

In addition to focusing on skin cancer, this study acknowledges the potential inclusion of other forms of cancer. Future iterations of the research may incorporate diverse classifications, extending beyond skin cancer, to encompass conditions such as dermatofibroma (DF) and basal cell carcinoma

(BCC). The objective of broadening the classification scope is to augment the adaptability of the model and foster a more all-encompassing comprehension of diverse dermatological ailments. This progression is consistent with the continuous progress in machine learning and medical imaging, promoting a more comprehensive and inclusive method of cancer identification and categorization.

REFERENCES

[1] Ferrante di Rufino L, et al. Computer-assisted diagnosis techniques(dermoscopy and spectroscopy-based) for diagnosing skin cancer in adults. Cochrane Database System Rev. 2018. https://doi.org/10.1002/14651858.CD013186.

[2] Dinnes J, et al. Reflectance confocal microscopy for diagnosing cutaneous melanoma in adults. Cochrane Database System Rev.2018. https://doi.org/10.1002/14651858.CD013190.

[3] CNN Architectures: LeNet, AlexNet, VGG, GoogLeNet, ResNet and more 2019. https://medium.com/@sidereal/cnns-architectures-lenet-alexnet-vgg-googlenet-resnet-and-more-666091488df5. Accessed 20 July 2019.

[4] Vatsala Singh and Ifeoma Nwogu, "Analysing Skin Lesions in Dermoscopy Images Using Convolutional Neural Networks", 2018 IEEE International Conference on Systems, Man, and Cybernetics

[5] Shetty, B., Fernandes, R., Rodrigues, A.P. et al. Skin lesion classification of dermoscopic images using machine learning and convolutional neural network. Sci Rep 12, 18134 (2022). https://doi.org/10.1038/s41598-022-22644-9

[6] Md. Kamrul Hasan, Md. Toufick E. Elahi, Md. Ashraful Alam, Md. Tasnim Jawad, Robert Martí, DermoExpert: Skin lesion classification using a hybrid convolutional neural network through segmentation, transfer learning, and augmentation, Informatics in Medicine Unlocked,Volume 28,2022,100819, ISSN 2352-9148, https://doi.org/10.1016/j.imu.2021.100819.

[7] Ahmadi Mehr R, Ameri A. Skin Cancer Detection Based on Deep Learning. J Biomed Phys Eng. 2022 Dec 1;12(6):559-568. doi: 10.31661/jbpe.v0i0.2207-1517. PMID: 36569567; PMCID: PMC9759648.

[8] Jasil, S.P.G., Ulagamuthalvi, V. A hybrid CNN architecture for skin lesion classification using deep learning. Soft Comput (2023). https://doi.org/10.1007/s00500-023-08035-w

[9] Zillur Rahman, Md. Sabir Hossain, Md. Rabiul Islam,Md. Mynul Hasan, Rubaiyat Alim Hridhee, An approach for multiclass skin lesion classification based on ensemble learning, Informatics in Medicine Unlocked,Volume 25,2021,100659,ISSN 2352-9148,https://doi.org/10.1016/j.imu.2021.100659.

[10] A. Afroz, R. Zia, A. O. Garcia, M. U. Khan, U. Jilani and K. M. Ahmed, "Skin lesion classification using machine learning approach: A survey," 2022 Global Conference on Wireless and Optical Technologies (GCWOT), Malaga, Spain, 2022, pp. 1-8, doi: 10.1109/GCWOT53057.2022.9772915.

[11] R D S, A S. Deep Learning Based Skin Lesion Segmentation and Classification of Melanoma Using Support Vector Machine (SVM). Asian Pac J Cancer Prev. 2019 May 25;20(5):1555-1561. doi: 10.31557/APJCP.2019.20.5.1555. PMID: 31128062; PMCID: PMC6857898.

[12] Zahra Mirikharaji, Kumar Abhishek, Alceu Bissoto, Catarina Barata, Sandra Avila, Eduardo Valle, M. Emre Celebi, Ghassan Hamarneh, A survey on deep learning for skin lesion segmentation, Medical Image Analysis, Volume 88,2023,102863, ISSN1361-8415, https://doi.org/10.1016/j.media.2023.102863.

[13] Di Ruano FL. Dermoscopy, with and without visual inspection, for diag-nosing melanoma in adults (review). Cochrane Libr Cochrane Database Systemhttps://doi.org/10.1002/14651858.CD011902.pub2

[14] Covalic ISIC 2017: skin lesion analysis towards melanoma International in ImagingCollaboration.

2017. https://challenge.kitware.com/#phase/584b0afccad3a51cc66c8e38. Accessed 12 May 2020.

[15] ADDI—Automatic computer-based Diagnosis system for Dermoscopy Images. https://www.fc.up.pt/addi/ph2 database.html. Accessed 24 July 2019.

[16] Smith LN. A disciplined approach to neural network hyper- parameters:part 1—learning rate, batch size, momentum, and weight decay. 2018. http://arxiv.org/abs/1803 09820. Accessed 19 July 2019.

[17] R. Bhavani, V. Prakash, R. Kumaresh, R. Srinivasan, Vision-based skin disease identification using deep learning, Int. J. Eng. Adv. Technol. (IJEAT) 8 (6) (2019), 3784–3788

[18] N. Hameed, A. Shabut, M.A. Hossain, A computer-aided diagnosis system for classifying prominent skin lesions using machine learning, in: 2018 10 th Computer Science and Electronic Engineering Conference, CEEC, Colchester, UK, 2019.

[19] N. Hameed, F. Hameed, A. Shabut, S. Khan, S. Cirstea, A. Hossain, An intelligent computer-aided scheme for classifying multiple skin lesions, Computers 62 (2019).

[20] S.A. AlDera, M.T.B. Othman, A model for classification and diagnosis of skin disease using machine learning and image processing techniques, Int. J. Adv. Comput. Sci. Appl. 13 (5) (2022).